Article:
Hussain, I, Kumi Barimah, E, Iqbal, Y et al. (2 more authors) (2019) Thermal, Mechanical and Optical Properties of TiO2-doped Sodium Silicate Glass-Ceramics. Transactions of the Indian Ceramic Society, 78 (3). ISSN 0371-750X

https://doi.org/10.1080/0371750X.2019.1626287

Thermal, Mechanical and Optical Properties of TiO_2-doped Sodium Silicate Glass Ceramics

Imtiaz Hussain[1,2], Eric K. Barimah[2], Yaseen Iqbal[1], Gin Jose[2], Raz Muhammad[3,*]

[1]Department of Physics, University of Peshawar, 25120, KP, Pakistan

[2]School of Chemical and Process Engineering, University of Leeds, LS2 9JT, UK

[3]Department of Physics, Abdul Wali Khan University Mardan, 23200 KP, Pakistan

*Email address: raz@awkum.edu.pk

Abstract

In this study, local mineral (silica sand) obtained from Hazara division; Khyber Pakhtunkhwa, Pakistan was fabricated into soda-lime silicate glass. Titanium dioxide (TiO_2) concentration in the range of 1-3 wt. % was added as a nucleating agent to investigate its effect on crystallization phase, density, hardness, thermal expansion coefficient (α), glass transition temperature (T_g), micro hardness and optical bandgap of soda lime silicate glass. XRD analysis revealed the formation of different crystalline phases such as cristobalite (SiO_2), wollastonite ($CaSiO_2$), and rutile (unrefined TiO_2, often with iron, F^{3+}) at different processing temperatures. The coefficient of thermal expansion and the optical gap energies varied from 72.5×10^{-7}/K to 77×10^{-7}/K and 3.71-3.93 eV with TiO_2 concentration, respectively. The mechanical properties were also in good agreement with those commercially used glass ceramics.

Keywords: Silica sand; Titanium oxide; Soda-lime silicate glass

1. Introduction

Silica sand is abundant in the earth crust and commonly used for making several base-glass and glass-ceramics materials. These glasses have a number of applications in construction and telecommunication industries [1], active and passive optical applications [2], and biomedical devices [3, 4]. Silicate glasses prepared using silica sand raw material obtained from different parts around the globe have been extensively studied, because of its high chemical resistance, low coefficient of thermal expansion high optical transparency [5, 6], mechanical strength, inexpensive raw materials used for fabrication, and solubility of transition metals [7-11]. The properties of the base-glass and glass-ceramics are strongly dependent on their composition and the presence of crystalline phases and glassy networks [12]. Hand et al. [13] studied the compositional effect of sodium-calcium-magnesium-silicate on its mechanical properties. It was found that glass transition temperature, hardness and density of the samples decreases by replacing CaO by MgO. Further investigation of glass with $75SiO_2$-$15Na_2O$-10CaO (in mol.%) composition also revealed a mechanical hardness of 4.91 GPa. Omer et al. [14] synthesized transparent sodium silicate glass from local minerals with hardness of 5.5 GPa. It was reported that the coefficient of thermal expansion (CTE) decreases by increasing SiO_2 content. In another study, Mosallam et al. [15] studied silicate glasses with different ZnO concentrations and found that replacing CaO by ZnO which resulted into decrease CTE.

The Control of crystal nucleation play an important role in advancing glass-ceramics for many novel applications. In the absence of a nucleating agent, most glass systems crystallize from the surface on heating; very few crystallize from the bulk. Mastelaro et al. [16] reported that surface and volume nucleation tendency depend on the local structure around (calcium and lead) the modifier cations and the developed crystalline phase. The nucleating agents help to promote crystallinity in the glass on re-heating [17]. The nature of the crystallinity and distribution of the crystalline phase(s) formed during crystallization process are dependent on

the type and amount of nucleating agent. Many researchers have used TiO_2 as a nucleating agent [17-20]. The addition of TiO_2 improves glass formations and stabilizes the glass structure [21]. Furthermore, it also increases the glass crystallization, which improves the mechanical properties of the glass. The presence of TiO_2 in glass-ceramics decreases the viscosity of the base glasses at high temperature and favours the nucleation and crystal growth [18]. Mukerjee et al. [20] studied the effect of TiO_2 in calcium aluminium silicate system. It was found that TiO_2 promote crystallization in this glass system and increase its hardness. There has been increasing interest in developing high strength glass that could be used to produce significantly lighter glass products. Previous studies indicate that attempts have been made to control the mechanical properties through composition variation. The results reported by Deriano et al. [22] and Hand and Tadjiev [23] indicate that fracture toughness can be improved by replacing the larger ionic radii and high coordination ions with smaller ones. The properties can be either improved by composition of the glass or by converting the glass to glass-ceramics by adding appropriate nucleating agents. Therefore, in the present work, the $70SiO_2$-$14Na_2O$-$10CaO$-$4Al_2O_3$ glass prepared using locally mined raw materials and converted into glass-ceramics using $xTiO_2$ (wt. %) as a nucleating agent. The crystallization kinetics were examined using X-ray powder diffraction (XRD) and differential thermal analysis (DTA). The effect of nucleating agent and heat-treatment on the mechanical and optical properties of the fabricated glass ceramics were examined.

2. Experimental Methods

Sodium silicate glasses were synthesized by using silica sand obtained from Hazara division in Pakistan. The silica sand (source of SiO_2) powders were initially analysed using X-ray fluorescence (XRF) to determine the percentage composition of each element present in it. Based on this silicate glass of the following compositions $70SiO_2$-$14Na_2O$-$10CaO$-$4Al_2O_3$ with different concentrations of $xTiO_2$ (where x = 0, 1, 2, 3 wt.%) were prepared. T0 (0 wt.% TiO_2),

T1 (1 wt.% TiO_2), T2 (2 wt.% TiO_2), and T3 (3 wt.% TiO_2) designated as silicate glass samples which contain different concentrations of the nucleating agent, respectively. The TiO_2 (rutile) of reagent grade was used as a nucleating agent. The purity of TiO_2 was 99.5% (Alfa Aesar) and particle size was 1-2 □m. A 30 g batch of each composition was weighed and mixed thoroughly. The well-mixed powders were melted in platinum crucible for 3 hrs in the temperature range of 1450-1550 °C, at a heating rate of 10 ºC/min. After melting, the samples were transferred to a preheated furnace of approximately to 80% of the corresponding T_g and left it to anneal for 2 hrs to remove internal stresses. Then the furnace was allowed to cool to room temperature. The molten glass was then poured into a steel mould and properly annealed in a pre-heated furnace at 450 °C for 2 hrs to ensure the removal of any leftover internal stresses.

The densities of all samples were measured using a high precision densitometer. The nucleation and crystallization temperature were determined using simultaneous thermal analysis (STA, 8000, PerkinElmer USA). Alumina crucibles were used with Al_2O_3 powder as reference material. The STA measurements were performed at a heating rate of 10 °C/min in dry nitrogen atmosphere with a flow rate of 20 ml/min. The micro hardness of the investigated glasses was obtained from measurements using a Vicker's micro hardness indenter (Wilson tukon 1202 knoop/vickers tester, USA). The samples were cut with slow speed diamond saw and then grounded and polished with diamond paste to get the required surface smoothness and flatness before indentation. The glass transition temperature (T_g) and the CTE were determined using DTA and glass dilatometer at a heating rate of 5 $Kmin^{-1}$ in air. The phase identification of as prepared (annealed) and post heat-treated samples were determined using Phillips X-ray diffractometer (Phillips X'pert diffractometer USA). UV/Vis/NIR Spectrophotometer (LAMBDA 950 PerkinElmer USA) was also used to measure the optical transmittance of the investigated samples.

3. Result and Discussion

3.1 Crystallization characteristics

Figure 1 shows the DTA curves of the samples where the endothermic peak centred at 590-620 °C temperature range corresponds to the glass transition temperature (T_g). It was observed that as the concentrations of TiO_2 increased from 0 wt.% to 3 wt.%, the T_g value increased from 596 °C (TiO_2 free) to 617 °C. Besides, exothermic peaks at 630-650 °C were also observed which may be attributed to a single-phase crystallization or transformation of the crystal structure. T1 glass is the only sample which exhibited a broad band exothermic outcome. In contrast, T2 and T3 glasses which contain high concentrations of TiO_2, have very small exothermic effects as depicted in Fig. 1. It was found that an increase in TiO_2 concentration leads to changes in both endothermic and exothermic peak temperatures. Furthermore, the densities of the crystallization peak temperatures gradually decreased as TiO_2 concentration increased, while endothermic dips tend to increase.

XRD pattern of the as prepared glasses confirm amorphous phase band around 25° as shown in Fig. 2. The sample T0 (TiO_2 free) is entirely amorphous; whereas those of TiO_2 doped glass samples are mixtures of amorphous and crystalline phases while the crystalline phases of T1, T2 and T3 occur at ~ 45° and 52° [24].

In order to study the effect of heat treatment on crystallization, all samples were heat-treated from room temperature to 850 °C and 950 °C at 10 °C/min heat rate, 5 hrs dwell time and then cooled down at a ramp rate of 1°C/min to room temperature. Figures 3 shows the XRD data of samples heat-treated at 850 °C and 950 °C. The XRD analysis of the crystalline products of the base glass (T0) at 850 °C revealed distinct intense reflections centred ~ 22º, 36º, and some other reflections. The dominant peaks were observed as major crystalline phase which corroborate with cristobalite (SiO_2) of a card number 01-073-9753. At 950 °C, similar intense

peaks were also identified in the parent glass. Besides cristobalite phase, the XRD patterns of 1, 2 and 3 wt.% concentrations of TiO_2 doped glasses also revealed two more additional crystalline phases at 850 °C and 950 °C heat-treated samples. Cristobalite and rutile (TiO_2, often with iron, F^{3+}) crystalline phases were identified in TiO_2 doped glasses for 850 °C heat treated sample, matched PDF#01-073-9753 and 04-014-1641 [20]. Furthermore, the XRD results of glass samples heat-treated at 950 °C revealed additional crystalline phase known as sodium calcium silicate (matched PDF# 00-023-0671) as shown in Fig. 3(b), which was not found in Fig. 3(a). Therefore, it was concluded that TiO_2 as a nucleating agent in sodium silicate glass has strong influence on the number of the crystalline phases that are produced on heat-treatment. It was noticed that for samples with 3 wt.% TiO_2, the rutile crystalline phase disappeared on heat treatment at 850 °C (Fig. 3(a)). The intensity of the peaks for samples heat-treated at 950 °C is about twice higher than those samples heat-treated at 850 °C. These samples heat treated can therefore be considered to be transformed to glass-ceramics.

3.2 Co-efficient of Thermal Expansion

Figure 4 shows the coefficient of thermal expansion (CTE) of the as prepared quenched samples and heat-treated (glass-ceramics) samples. CTE increased with increasing temperature in both as prepared and the glass-ceramics samples heat-treated at 850 °C. The glass-ceramic samples showed lower CTE values in comparison to the as prepared glass samples. Furthermore, addition of TiO_2 as a nucleating agent leads to decrease in the CTE values of glass-ceramic samples as compared to TiO_2 free sample (T0). This decrease in CTE values from 77×10^{-7}/K to 72.5×10^{-7}/K may be attributed to the formation of crystal phases such as cristobalite and rutile in the heat-treated samples. Shelistak et.al [25] reported the CTE of the soda-lime glass as 92×10^{-7}/K. CTE value obtained for cristobalite phase is ~26.0×10^{-7}/K; therefore, the decrease in CTE of the heat-treated sample may be attributed to the formation cristobalite phase, as evident from XRD data.

3.3 Microhardness and density

Mechanical properties of material play a vital role towards its application. Hardness, which is the resistance of the materials to permanent deformation, is an important mechanical property of materials [24]. Vicker's hardness test is a suitable method for hardness measurement. A Wilson hardness equipped with Vicker's and Knoop indenters was used to determine microhardness, fracture toughness, and brittleness in this work. Several indentations were performed to measure hardness by varying the working loads from 50 g to 1000 g at a constant dwell time of 10 second. The samples were kept in desiccators for 24 h after indentation to enable the residual stresses to be released.

Ten indentations were measured for each load and the average value of average diagonal length (d) was recorded. Vicker's hardness number (H_v) was then obtained by using equation (1) [13]:

$$Hv = \frac{1.8544P}{d^2} \text{ ---------- (1)}$$

where 'P' is the applied load and 'd' is the average diagonal length.

Optical microscope (Olympia) was used to measure the total crack length (2c). The fracture toughness (K_{Ic}) was evaluated using Evans and Charles relation [13]:

$$K_{IC} = \frac{0.0824P}{c^{3/2}} \text{ ---------- (2)}$$

Brittleness was formulated as the ratio of the hardness to toughness as shown in equation (3) below

$$B = \frac{Hv}{K_{IC}} \text{ ---------- (3)}$$

Figure 5 shows optical microscope images of the indentation showing cracks emanated on the un-heat treated and heat-treated glass. The microhardness increased with increasing applied load which indicated the presence of the reverse indentation size effect [26]. As clear from Fig. 5(a) and (b), the heat-treated samples generated more permissible indentation cracks. This is due to change in the mechanical properties [27] of the heat-treated samples such as hardness,

fracture toughness and brittleness. Kilinc et.al [28] studied the soda-lime silica glasses and reported that the mechanical properties of the investigated glasses improved with increasing alkaline earth content and reported the maximum hardness to be 5.96 GPa and the brittleness as 6.0 $\mu m^{-1/2}$. Hand and Tadjiev [13] also studied NCMS (Sodium Calcium Magnesium Silicate) glasses as a function of composition and reported their hardness as 4.91 GPa) and brittleness as 6.82 $\mu m^{-1/2}$. Wu et.al [29] studied glass-ceramics containing high TiO_2 contents and reported that the crystallization of the glass yielded better mechanical properties than the parent glass. In the present study, the hardness of the T3 sample was ~5.6 GPa and brittleness was 5.52 $\mu m^{-1/2}$. Upon crystallization the hardness was observed to increase to ~6.2 GPa and the brittleness decreased to 4.87 $\mu m^{-1/2}$. The increase in the hardness of heat-treated samples may be attributed to the formation of cristobalite stable phase during the nucleation process. The progress of crystalline phases increases the connectivity, which shows more resistance to deformation, and may enhance hardness. Table I illustrates the values of hardness, fracture toughness, brittleness and densities for all the samples. It can be seen that the observed hardness of the samples increased with increasing concentrations of TiO_2, as well as heat treatment.

3.4 UV-Vis-NIR spectroscopy

The UV-Vis transmission spectra of the prepared samples before and after heat treatment are shown in Fig. 6. The spectra showed a good transmission around ~ 72 % and above for glasses before heat treatment. As the doping concentrations of TiO_2 in the glasses increased from 1 to 3 wt.%, the transmission decreased slightly as depicted in the Fig 6(b). The UV-Vis studies of as prepared samples revealed some weak absorption bands at ~ 378 nm, 444 nm and 484 nm which may be attributed to ferric iron (Fe^{3+}) and TiO_2 nanoparticles presence in these glasses [30]. All these identified absorption peaks are consistent with the rutile crystalline phase [30], consistent with the XRD data. The overall transmission of glasses heat treated at 800 °C decreased and this may be due to the formation of micro-crystallites and the transformation of

glasses to glass-ceramics. This also led to the disappearance of the absorption bands due to the absence of nanocrystalline phases, as shown in Fig. 6(b).

The optical band gap energy of un-doped and TiO_2 doped glasses were calculated from the UV absorption edge using Mott and David's relation for amorphous materials [31]:

$$\alpha h\nu = B^2\left(h\nu - E_g\right)^2 \text{ ---------- (4)}$$

where 'α' is absorption coefficient, $h\nu$ is the energy of incident photons, E_g is the optical band gap, 'B' is the band tailing forbidden and 'm' is the different transition states. It is known that amorphous materials are best fitted with m = 2 in equation (4).

Nocun et. al. [32] studied that; prolonged annealing time increases energy band gap. They also reported that TiO_2 crystal growth may also increase the energy band gap. Ali et.al [33] studied the band gap energy of the soda-lime glass doped with ZnO. They reported an increase in E_g with increasing ZnO concentration.

Refractive index of TiO_2 doped glasses before and after heat-treatment were calculated using the relation (5)

$$\frac{n^2-1}{n^2+2} = 1 - \sqrt{E_g/20} \text{ ------(5)}$$

Salih et.al [33] reported that the addition of ZnO to Soda-lime glass may increase the refractive indices of the resulting glasses. This might be due to the fact that ZnO generates more non-bridging oxygen's in the network. Tan et. al. [34] studied the silica glass and reported that the refractive index increased with increasing density. The higher refractive index of 1.53 was reported for the samples with 2.58 g/cm^3 density.

The optical band gap and refractive indices of all the investigated samples before and after heat-treatment are given in Table II. The refractive index and optical energy band gap of the samples before and after heat-treatment varied in range 2.181 ~ 2.189 and 3.90 ~ 3.93 eV and 2.211 ~ 2.228 and 3.71 ~ 3.79 eV respectively. The optical energy band gap decreased by a small amount as the concentration of TiO_2 increased from 1 to 3 wt.% in both before and after

heat-treated samples. This decrease in band gap may be due to increase in bonding defect and non-bridging oxygen's (NBO) [31].

4. Conclusions

Different batches of sodium silicate glass were prepared from a locally available raw material such as silica sand from Hazara division, Khyber Pakhtunkhwa, Pakistan. The base glass was modified by adding nucleating agent TiO_2 with different concentrations. Studies were conducted to evaluate the effect of different concentrations of TiO_2 and heat treatment on the crystallization, coefficient of thermal expansions, hardness, and optical properties of the as prepared glass and glass ceramics. Differential thermal analysis showed slight change in the transition temperature (T_g) ranging from 590 to 620^oC and exothermic peaks shift from 630 to 650$^{\circ}C$. XRD measurements of the parent glass revealed the presence of cristobalite (SiO_2) as the main crystalline phase. The cristobalite and rutile phases were also observed at high temperature in glass samples doped with TiO_2 nucleating agent and the crystallinity increased with increase in temperature. The analyses conducted with as prepared and heat-treated samples revealed net increased in hardness. The coefficient of thermal expansion also increased with increase in concentration of nucleating agent. This study shows that the transmittance as well as the energy band gap of the samples decreased by converting parent glass to glass ceramics. A good combination of mechanical properties was achieved for these samples.

Acknowledgment

The author (Imtiaz Hussain) acknowledge the Higher Education Commission of Pakistan for the award of research fellowship under the International Research Support Initiative Program (IRSIP) at the University of Leeds, UK.

References

1. W. Höland, V. Rheinberger, E. Apel, C. van't Hoen, M. Höland, A. Dommann, M. Obrecht, C. Mauth, U. Graf-Hausner, J. Mater. Sci.:Mater. Electron., **17**, 1037-1042 (2006).
2. I. Alekseeva, O. Dymshits, M. Tsenter, A. Zhilin, V. Golubkov, I. Denisov, N. Skoptsov, A. Malyarevich, K. Yumashev, J. Non-Cryst. Solids, **356**, 3042-3058 (2010).
3. W. Vogel, J. Non-Cryst. Solids, **73**, 593-597 (1985).
4. W. Vogel, W. Hoeland, K. Naumann, J. Gummel, J. Non-Cryst. Solids, **80**, 34-51 (1986).
5. H. Park, S. Lee, B. Ryu, M. Son, H. Lee, I. Yasui, J. Mater. Sci., **31**, 4249-4253 (1996).
6. N.P. Padture, H.M. Chan, J. Am. Ceram. Soc., **75**, 1870-1875 (1992).
7. A. Paul, A. Youssefi, J. Mater. Sci., **13**, 97-107 (1978).
8. D.M. Teter, MRS Bull., **23**, 22-27 (1998).
9. S. Ronchin, R. Rolli, M. Montagna, C. Duverger, V. Tikhomirov, A. Jha, M. Ferrari, G. Righini, S. Pelli, M. Fossi, J. Non-Cryst. Solids, **284**, 243-248 (2001).
10. H. Wang, G. Henderson, Chem. Geol., **213**, 17-30 (2004).
11. P. Chimalawong, J. Kaewkhao, C. Kedkaew, P. Limsuwan, J. Phys. Chem. Solids, **71**, 965-970 (2010).
12. V. Marghussian, M.D. Niaki, J. Eur. Ceram. Soc., **15**, 343-348 (1995).
13. R.J. Hand, D.R. Tadjiev, J. Non-Cryst. Solids, **356**, 2417-2423 (2010).
14. O.A. Al-Harbi, M.M. Khan, Trend. Appl. Sci. Res., **4**, 176-187 (2009).
15. H. Abo-Mosallam, H. Darwish, S. Salman, J. Mater. Sci.:Mater. Electron., **21**, 889-896 (2010).
16. V.R. Mastelaro, E.D. Zanotto, N. Lequeux, R. Cortes, J. Non-Cryst. Solids, **262**, 191-199 (2000).
17. L. Barbieri, A.B. Corradi, C. Leonelli, C. Siligardi, T. Manfredini, G.C. Pellacani, Mater. Res. Bull., **32**, 637-648 (1997).

18. X. Tan, S. Liang, R. Liu, D. Guan, L. Chai, Phase Transit., **84**, 1035-1044 (2011).

19. J.-J. Shyu, J.-M. Wu, J. Mater. Sci. Lett., **10**, 1056-1058 (1991).

20. M. Chavoutier, D. Caurant, O. Majérus, R. Boulesteix, P. Loiseau, C. Jousseaume, E. Brunet, E. Lecomte, J. Non-Cryst. Solids, **384**, 15-24 (2014).

21. S. Abdel-Hameed, M. Azooz, Ceram. Int., **35**, 643-648 (2009).

22. S. Deriano, T. Rouxel, M. LeFloch, B. Beuneu, Physics and Chemistry of Glasses, **45**, 37--44 (2004).

23. R.J. Hand, D.R. Tadjiev, Journal of Non-Crystalline Solids, **356**, 2417-2423 (2010).

24. K. Keong, W. Sha, S. Malinov, Surf. Coat. Tech., **168**, 263-274 (2003).

25. L. Shelestak, R. Chavez, J. Mackenzie, B. Dunn, Journal of Non-Crystalline Solids, **27**, 75-81 (1978).

26. S. Sagadevan, S.S. Anandan, Int. J. Mater. Eng., **4**, 70-74 (2014).

27. W. Pannhorst, J. Non-Cryst. Solids, **219**, 198-204 (1997).

28. E. Kilinc, R.J. Hand, Journal of Non-Crystalline Solids, **429**, 190-197 (2015).

29. J.P. Wu, R.D. Rawlings, A.R. Boccaccini, I. Dlouhy, Z. Chlup, Journal of the American Ceramic Society, **89**, 2426-2433 (2006).

30. B. Mehdikhani, G.H. Borhani, Process. Appl. Ceram., **7**, 117-121 (2013).

31. S. Ruengsri, J. Kaewkhao, P. Limsuwan, Procedia Engineer., **32**, 772-779 (2012).

32. M. Nocun, S. Kwaśny, J. Zontek, Optica Applicata, **41**, 979-987 (2011).

33. A.S. Ali, M.D. Abdalla, M. Adam, Y.I. Elawad, Alsalam university Journal, **7**, 61-72 (2018).

34. C. Tan, J. Arndt, H. Xie, Physica B: Condensed Matter, **252**, 28-33 (1998).

List of Tables

List of Figures

Table I

No		Before heat treatment				After heat treatment		
Sample	ρ (g/cm^3)	Hv (GPa)	K_{Ic} ($MNm^{-3/2}$)	B ($\mu m^{-1/2}$)	ρ (g/cm^3)	Hv (GPa)	K_{Ic} ($MNm^{-3/2}$)	B ($\mu m^{-1/2}$)
T0	2.45	5.093	0.87±0.1	5.85±0.1	2.38	5.28	1.03±0.01	5.11±0.01
T1	2.48	5.278	0.93±0.1	5.67±0.1	2.35	5.69	1.13±0.01	5.03±0.01
T2	2.53	5.353	0.97±0.1	5.52±0.1	2.32	6.00	1.23±0.01	4.88±0.01
T3	2.54	5.578	1.01±0.1	5.52±0.1	2.31	6.18	1.27±0.01	4.87±0.01

Table II

TiO_2 Concentration (wt. %)	Band Gap Energy (eV) Before Heat-treated	Band Gap Energy (eV) After Heat treated	Refractive Index (n)	
			Before Heat-treated	After Heat-treated
0.0	3.93	3.79	2.181	2.211
1.0	3.92	3.75	2.183	2.220
2.0	3.91	3.72	2.184	2.226
3.0	3.90	3.71	2.189	2.228

Fig. 1

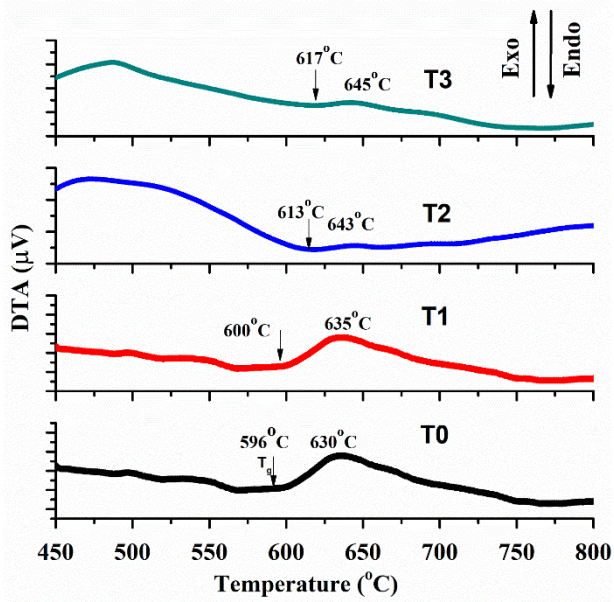
617°C
645°C
T3
Exo
Endo
613°C
643°C
T2
DTA (μV)
600°C
635°C
T1
596°C
630°C
T0
Tg
450
500
550
600
650
700
750
800
Temperature (°C)

Fig. 2

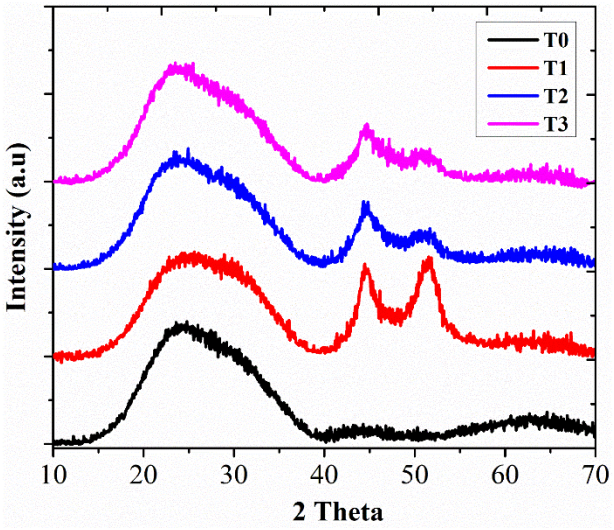
T0
T1
T2
T3
Intensity (a.u)
10
20
30
40
50
60
70
2 Theta

Fig. 3

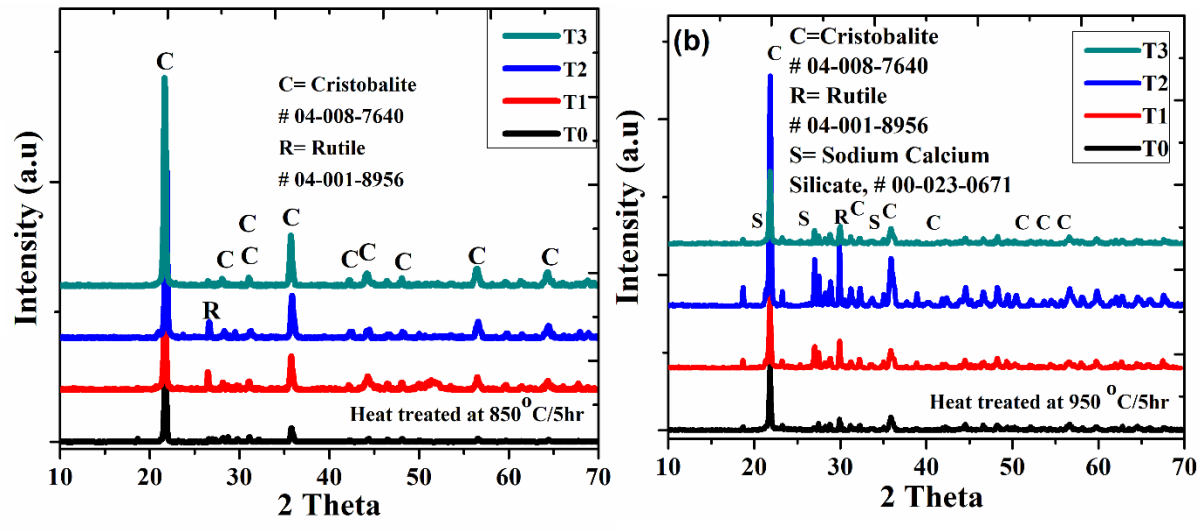

Fig. 4

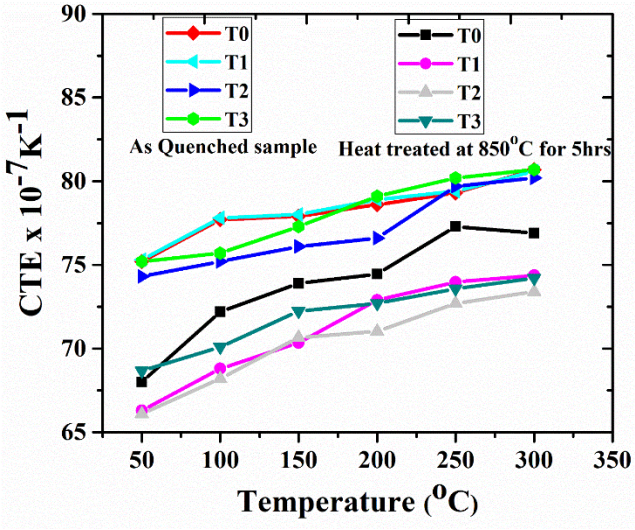

Fig. 5

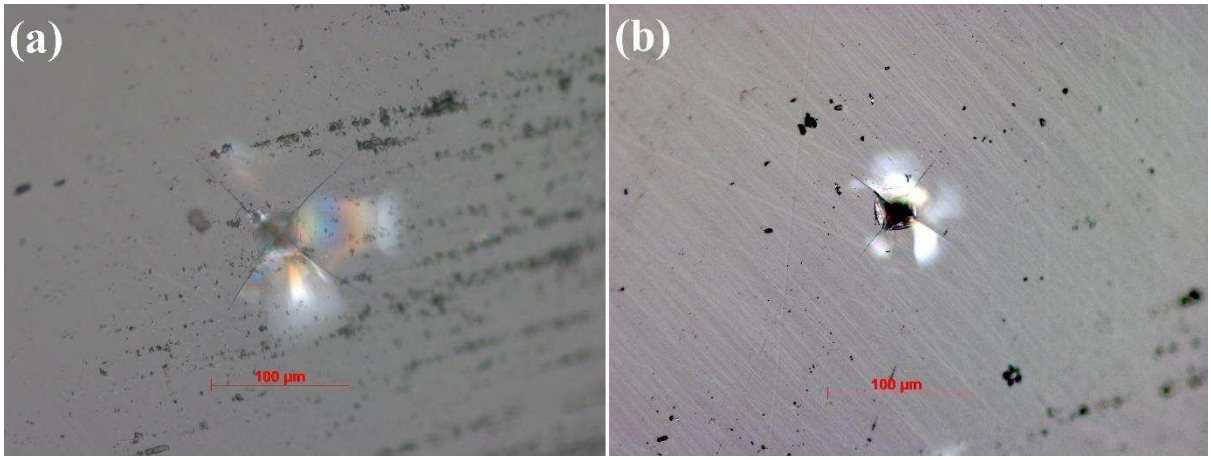

Fig. 6

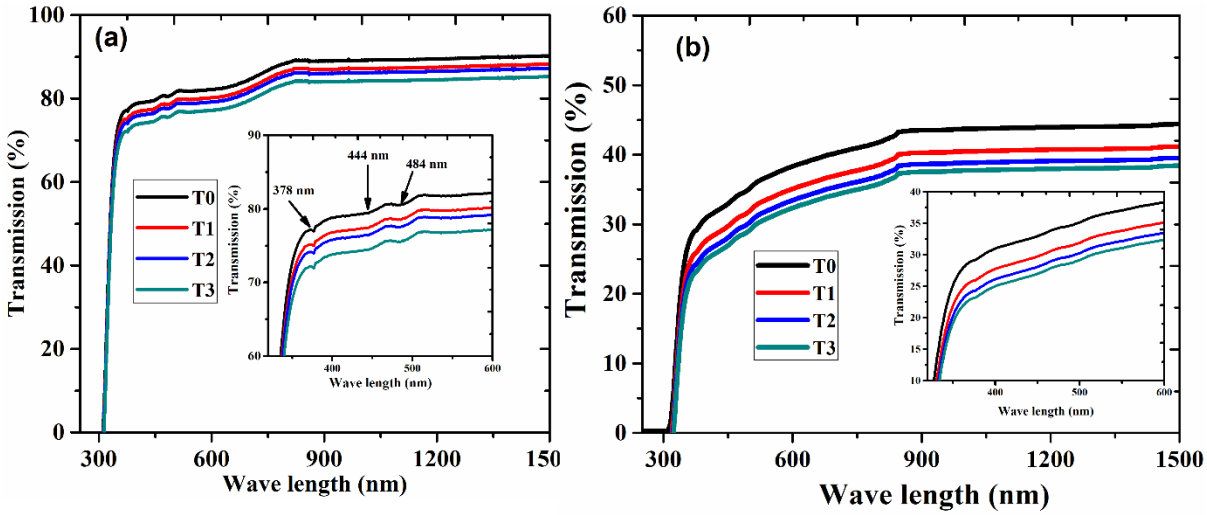
(a)
Transmission (%)
Wave length (nm)
T0
T1
T2
T3
378 nm
444 nm
484 nm
(b)
Transmission (%)
Wave length (nm)
T0
T1
T2
T3